Accepted Manuscript

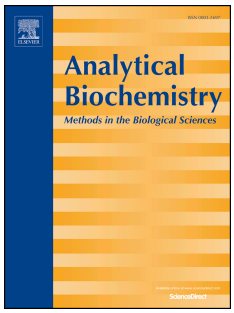

Acetylcholinesterase biosensor based on functionalized surface of carbon nanotubes for monocrotophos detection

Zou Bin, Chu Yanhong, Xia Jiaojiao, Yao Jing

PII: S0003-2697(18)30415-9

DOI: 10.1016/j.ab.2018.08.024

Reference: YABIO 13119

To appear in: *Analytical Biochemistry*

Received Date: 16 April 2018

Revised Date: 27 August 2018

Accepted Date: 28 August 2018

Please cite this article as: Z. Bin, C. Yanhong, X. Jiaojiao, Y. Jing, Acetylcholinesterase biosensor based on functionalized surface of carbon nanotubes for monocrotophos detection, *Analytical Biochemistry* (2018), doi: 10.1016/j.ab.2018.08.024.

Acetylcholinesterase biosensor based on functionalized surface of carbon nanotubes for monocrotophos detection

Zou Bin *, Chu Yanhong, Xia Jiaojiao*, Yao Jing

School of Food and Biological Engineering,

Jiangsu University, Zhenjiang, 212013, China.

Abstract

Monocrotophos (Ops) has been widely used as pesticide in crop production but simultaneously could accumulate in the nature and seriously impact food safety and human health. It is necessary to develop a high sensitivity biosensor for accurate and fast detection of OPs. In this study, multi-walled carbon nanotubes (MWCNTs) were selected as acetylcholinesterase (AChE) carrier and their surface was modified by introducing different functional groups (-SH, -NH_2, -Cl, -OH), hydrophobic alkyl groups (-CH_3, -$(CH_2)_2CH_3$, -$(CH_2)_7CH_3$, -$(CH_2)_{15}CH_3$) and ionic liquids (-IL_1, -IL_2). The interaction mechanism of MWCNTs functionalized surface and AChE has been revealed by studying characteristics of AChE immobilized on different carrier surface. Finally, compared with reported references and above other modifiers, we found that MWCNTs surface modified by -IL_1 was the best carrier for AChE and the detection limit of IL_1-MWCNTs/AChE/GCE was 3.3×10^{-11} M. At optimum reaction condition (pH 7.0, AChE loading 0.25 U, Inhibition time 14 min), storability test indicated reactivity of IL_1-MWCNTs/AChE/GCE remained above 98.5% within two weeks. For real vegetable sample detection, the recoveries of IL_1-MWCNTs/AChE/GCE were found to be between 90.0% and 104%. These results demonstrated novel biosensors could act as device of high sensitivity for accurate and fast detection of OPs.

Keywords: monocrotophos, acetylcholinesterase, enzyme electrode, carbon nanotubes, surface modification

* To whom correspondence should be addressed. The postal address: Jiangsu University, No. 301 Xuefu Road, Zhenjiang 212013, China. Tel/Fax.: +86-0511-88780201; E-mail: Binzou2009@ujs.edu.cn. Jiaojiaoxia@ujs.edu.cn

1. Introduction

Monocrotophos (OPs) is extremely toxic for pests, wherein it causes irreversible phosphorylation of esterase, hinders transport of neurotransmitter choline and affects function of central nervous system. Hence, it has been widely used as a pesticide in crop production [1, 2]. However, OPs toxic residues could accumulate in the nature, and cause serious impact on food safety and human health. Therefore, lot of attention has been given to OPs toxic residues in the food.

Compared to liquid or gas phase chromatography, electrochemical sensors are currently favored for detecting OPs residues by majority of researchers due to its speed, accuracy and convenience. There are numerous electrochemical methods, such as non-enzyme electrode method [3], electrochemical biosensor [4], electrochemical molecular imprinting [5], electrochemical luminescence [6], capillary electrophoresis [7] etc. However, electrochemical biosensor is most prominently used for OPs detection. It fixes molecular recognition substances such as enzymes [8], antigens/antibodies [9], DNA [10] on transducers, and converts the concentration signal of substrate into an electrical signal. Compared to antigen/antibody or DNA, acetylcholinesterase (AChE) biosensor is simpler, faster and most cost-effective molecular recognition substance. It provides high sensitivity signal and is most likely tool to be used for rapid detection of OPs in industry.

Excellent AChE sensor not only maintains AChE activity, but also enhances the enzyme activity by adjusting the surface of immobilized carrier [11]. Therefore, performance of AChE primarily depends on the design of immobilized carrier

construct and surface. MWCNTs have been extensively applied in enzyme immobilization and electrochemistry due to its porous hollow structure, huge surface, and unique hydrophobic properties [12]. However, surface of original MWCNTs does not carry any polar groups except for -OH. Chemical modification of surface could change the microenvironment of enzyme and improve activity of AChE. Kang et al. showed that when AChE is immobilized on grapheme oxide (GO) with phenoxy-modified dextran through hydrophobic interaction, the function of GO has been improved. A novel OPs biosensor has been created and detection limit was 28.55 M paraoxon [13].

Surface properties of carrier have significant impact on the performance of the AChE sensor. However, at present, sensitivity of modified electrode was still not high enough for detecting OPs. In addition, modifiers usually just focused on single functional group. There is no methodical research and in-depth discussion about the influence of different carrier surface on performance of AChE. In this study, the MWCNTs selected as AChE carrier were modified by introducing different functional groups (-NH_2, -SH, -OH, -Cl), hydrophobic alkyl groups (-CH_3, -$(CH_2)_2CH_3$, -$(CH_2)_7CH_3$, -$(CH_2)_{15}CH_3$) and ionic liquids (IL_1, -IL_2). These different groups were typical representative of functional group, hydrophobicity group and ionic groups. Expanded novel modifier of MWCNTs such as –SH, -$(CH_2)_7CH_3$ and ionic liquid has been used to improve AChE performance for the first time. Impact of different surface materials on biosensor and mechanism of interaction between surfaces and AChE were explored under optimized experimental conditions (pH, enzyme loading on the

biosensor, inhibition time). Overall, these novel biosensors act as high sensitivity device for detection of OPs and are expected to lay a foundation for accurate and fast detection of OPs.

2. Experimental

2.1 Reagents and materials

Trimethoxy(methyl)silane, trimethoxy (propyl) silane, trimethoxy (octyl) silane, trimethoxy(hexadecyl)silane, (3-aminopropyl) trimethoxysilane, (3-chioropropyl) trimethoxysilane, (3-mercaptopropyl) trimethoxysilane and 1-methylimidazole were purchased from Shanghai Aladdin Biochemical Technology Co., Ltd. Phosphate buffer (PBS) was prepared by mixing NaH_2PO_4 and Na_2HPO_4 in different proportions. MWCNTs (Purity＞95%, Length 0.5-2 μm, OD＞50 nm, OH-MWCNTs) were purchased from Beijing Deke Island Gold Technology Co., Ltd. OPs (99.4%) were obtained from Beijing Putian Tongchuang Biotechnology Co., Ltd. (China). Acetylcholinesterase (AChE, Type C3389, 500 U mg^{-1} from electrophorus electricus) and acetylthiocholine chloride (ATCl) were purchased from Sigma-Aldrich (USA). Sodium tetrafluoroborate ($NaBF_4$) was purchased from Shanghai Sain Chemical Technology Co., Ltd. The other reagents were analytical grade and used without further purification. Double distilled water was used in all experiments.

2.2 Preparation of modified carrier

1 g MWCNTs-OH powder was weighed into flask containing 100 mL chloroform. Uniform black MWCNTs-OH solution was obtained after ultrasound for 15 minutes. And then 10 mmol reagent (trimethoxy(methyl)silane, trimethoxy(propyl)silane,

trimethoxy(octyl)silane, trimethoxy(hexadecyl)silane, (3-aminopropyl) trimethoxysilane, (3-mercaptopropyl)trimethoxysilane or (3-chioropropyl) trimethoxysilane was added to flasks. The mixture was stirred for 5 days at 25 □ on a stirrer. The synthesized black solution was filtered, washed and dried in an oven at 80 □ for 5 hours. The composites were referred to as C_1-MWCNTs, C_3-MWCNTs, C_8-MWCNTs, C_{16}-MWCNTs, NH_2-MWCNTs, SH-MWCNTs, Cl-MWCNTs, respectively (**Scheme 1**) [14].

Preparation of MWCNTs modified by ionic liquids is show below. Equimolar 1-methylimidazole and (3-chioropropyl) trimethoxysilane were first stirred at 95 □ for 24 h. Chloride ionic liquid (IL_1) was obtained. Loaded chloride ionic liquid (10 mmol/g) was obtain according to above reaction processes and referred to as IL_1-MWCNTs (**Scheme 2**). 1 g IL_1-MWCNTs were weighed into a conical flask. 10 mmoL $NaBF_4$ and 100 mL distilled water was added. Borofluoride ionic liquid modified MWCNTs (IL_2-MWCNTs) was obtained after stirring at 25 □ for 5 days [15].

2.3 Preparation of modified electrode

Standard counter electrode (platinum wire electrode) and reference electrode (Ag/AgCl electrode) were used in this process. The electrodes were polished with 0.10 μm and 0.05 μm alumina slurry, and then ultrasonically cleaned in water for 15 minutes. 10 mg carrier material was weighed and dissolved in 1 mL PBS buffer (pH 7.0). The dispersive carrier solution was prepared after ultrasound for 15 minutes. 5 mg enzyme was weighed and dissolved in 60 mL Tris-HCl (pH 7.0). The enzyme

solution was obtained after ultrasound for 15 minutes. 10 uL carrier solution dropped on bare electrode surface with pipette. The electrodes were then dried with an infrared lamp for 20 minutes. After that, 10 μL enzyme solution was placed on the surface of the carrier. After dried, the modified electrode used in the experiment was synthesized (**Scheme 3)**. The electrodes need be stored in a refrigerator with 0-4 □.

2.4 Electrochemical detection of OPs

The biosensor was employed for determination of OPs using DPV method. The performance of biosensor was tested by its DPV response in pH 7.0 PBS solution containing 1.0 mmol/L ATCl. Then the electrode was rinsed with PBS (pH 7.0) and incubated in an aqueous solution containing the desired concentration(1×10^{-10}, 5×10^{-10} , 1×10^{-9}, 5×10^{-9}, 1×10^{-8}, 5×10^{-8}, 1×10^{-7}, 5×10^{-7} M) of OPs. Finally, it was transferred into ATCl solution for DPV measurements at the same condition of OPs inhibition absence. The inhibition rate of OPs was calculated as follows:

$$I(\%) = \frac{i_1 - i_2}{i_1} \times 100\%$$

Where i_1 was the peak current of ATCl on biosensors without OPs inhibition, i_2 was the peak current of ATCl on biosensors with OPs inhibition. I was inhibition rate and was plotted against the concentrations of OPs to obtain linear calibration graphs. .

2.5 Apparatus and characterization method

Fourier transform-infrared (FT-IR) measurements were recorded using a Nicolet-460 FTIR spectrometer with a spectral resolution of 0.4 cm^{-1} in the wave number range of 500-4000 cm^{-1}. Thermogravimetry (TG) was obtained using a Rheometric Scientific STA1500 analyzer at the temperature from 200-1000 □ in

nitrogen atmosphere to verify the property of carrier under thermogravimetric analysis. Cyclic voltammetry (CV) and different pulse voltammetry (DPV) measurements were performed with CHI660 D electrochemical workstation (Shanghai Chenhua Co., Ltd. China). All experiments were performed with a three-electrode system (Glass electrode (GCE) for the working electrode, Ag/AgCl electrode as the reference electrode, platinum wire electrode for the detecting electrode) at room temperature.

2.6 Preparation of real sample solution

Fresh potted plants were purchased in the local supermarket. The potted leaves were cleaned using distilled water and then dried naturally. Different concentrations of OPs standard solution were sprayed to the fresh leaves. After 24 hours， the leaves were removed and crushed. Each sample was added by 10 mL 0.1 mol L^{-1} pH 7.0 PBS and sonicated for 3 minutes. In the absence of extraction or pre-concentration of the case, the samples were directly detected by DPV method. The concentration of the OPs contained in the sample was obtained directly by the calibration curve.

3. Results and discussion

3.1 Electrochemical behavior of the biosensors

After introducing different modified materials, nature of MWCNTs has been changed differently. In this study, the modified electrode was scanned by differential pulse in pH-7.0 PBS containing 1.0 mmol L^{-1} ATCl to obtain DPV curve. The results were shown in **Fig. 1**. Peak current values of C_1-MWCNTs/AChE/GCE, C_3-MWCNTs/AChE/GCE, C_8-MWCNTs/AChE/GCE and C_{16}-MWCNTs/AChE/GCE were 2.348, 4.001, 5.146 and 3.445 uA, respectively. The results showed that the effect of C_8-MWCNTs was the best among four different hydrophobic alkanes (**Fig. 1**

A). Alkane chains were hydrophobic and could act near the active center of AChE as a conductor connecting the substrate to the active site of the enzyme. It was demonstrated that proper length of carbon chain facilitated activity express of AChE. Peak current values of SH-MWCNTs/AChE/GCE, NH_2-MWCNTs/AChE/GCE and Cl-MWCNTs/AchE/GCE were 3.858, 2.311 and 1.146 uA, respectively. The response of SH-MWCNTs modified GCE was relatively higher among different modified groups (**Fig. 1 B**). It was deduced that S-S has been formed between mercapto groups, and a network structure was built inside MWCNTs. AChE was immobilized on MWCNTs under the influence of S-S network, which probably increased the sensor stability and electrochemical performance [16]. But the peak values of SH-MWCNTs was lower than C_8-MWCNTs/AChE/GCE due to weak hydrophobicity. Peak current values of IL_1-MWCNTs/AChE/GCE and IL_2-MWCNTs/AChE/GCE were 6.845 and 5.311 uA, respectively. The performance of IL_1-MWCNTs and IL_2-MWCNTs was better than other composites due to ionic introducing (**Fig. 1 C**). It was shown that materials of C_8-MWCNTs, SH-MWCNTs, IL_1-MWCNTs effectively improved the sensitivity of the electrode, increased the current response value, promoted the progress of the reaction, and was more suitable for the detection of OPs.

CV was used to compare the electrochemical behavior of different carrier materials. CVs of bare GCE, MWCNTs/GCE, C_8-MWCNTs/GCE, SH-MWCNTs/GCE and IL_1-MWCNTs/GCE in 0.1 M PBS (pH 7.0) containing 5.0 mmol $L^{-1}[Fe(CN)_6]^{3-/4-}$ and 0.1 mol L^{-1} KCl were recorded. As shown in **Fig. 2**, there was a pair of well-defined redox peaks observed on the bare GCE (**Fig. 2 a**). The peak currents of the

MWCNTs/GCE (**Fig. 2 b**) increased since the good electrical conductivity and enhanced surface area of MWCNTs, the peak current was about 20 uA. Redox peaks of SH-MWCNTs/GCE, C_8-MWCNTs/GCE, IL_1-MWCNTs/GCE were relatively higher (**Fig. 2 c, d, e**). The highest redox peaks were appeared at the IL_1-MWCNTs/GCE. Due to the special electrochemical properties, the peak current was highest and about 30 uA corresponding to DPV results. It was demonstrated that IL_1-MWCNTs/GCE was the best carrier for AChE which consisted with above DPV results of IL_1-MWCNTs/AChE/GCE [17].

3.2 Characterization of prepared materials

TEM images of original MWCNTs (A, C) and IL_1-MWCNTs (B, D) were shown in Fig. 3. The MWCNTs before and after modification was well dispersed. However, Fig. 3D showed that the modification of ionic liquid has enabled MWCNTs to disperse more homogenously. It can be seen that surface and channel of MWCNTs after modification was vague. It demonstrated ionic liquid was grafted onto MWCNTs successfully. FTIR was performed to characterize group introducing results of MWCNTs, C_8-MWCNTs, SH-MWCNTs and IL_1-MWCNTs (**Fig. 4**). The FTIR spectrum of MWCNTs (**curve a**) displayed the presence of O-H (3430 cm^{-1}), C-C (1620 cm^{-1}) and C-O (1047 cm^{-1}), which was ascribed to the stretching vibrations of MWCNTs [18]. In addition to the presence of the characteristic peaks of MWCNTs, a new characteristic peak of C_8-MWCNTs (**curve b**) appears compared with MWCNTs. $-CH_2-$ (2960 cm^{-1}, 2870cm^{-1}) and $-CH_3$ (2930 cm^{-1}, 2850 cm^{-1}) were ascribed to the stretching vibrations of carbon chain (octyl). It was indicated that the surface carbon chains had been successfully attached to MWCNTs. The infrared band at 2500~2600

cm^{-1} was referred to S-H stretching vibration [19], which were characteristic in SH-MWCNTs (curve c). The characteristic peak near 3000 cm^{-1} was the stretching vibration of the unsaturated C-H bond. The absorption peak of 1640$cm^{-1}$and 1580 cm^{-1} were telescopic vibration on the imidazole ring of ionic liquid. 1450 cm^{-1} was the N-H bond bending vibration. These absorption peaks represented that IL_1-MWCNTs (curve d) had been synthesized. Compared with curve a, the characteristic peaks of -OH in the curves b, c and d were obviously weakened, which meant that the hydroxyl groups on MWCNTs were replaced by other groups.

TG was the weight loss curve of the sample during heating [20]. **Fig. 5** showed the TG analysis of all MWCNTs sample before and after modification. According to the quality change, the amount of modified materials could be calculated. The TG curve was divided into three stages. The first stage below 200 °C was mainly the evaporation of water. The second stage was the loss of MWCNTs groups, such as carbon chains, mercapto groups and ionic liquids. The third stage was the loss of the loaded AChE. According to the quality change, the loading of octyl, mercapto and chloride ionic liquids could be calculated as 42.5, 113.2 and 137 mg g^{-1}, respectively, and the loading of AChE in C_8-MWCNTs/AChE/GCE, SH-MWCNTs/AChE/GCE and IL_1-MWCNTs/AChE/GCE were 123.5, 108.3 and 215.1 mg g^{-1}, respectively.

3.3 Optimization condition of Biosensor Performance

The effect of solution pH on biosensor performance was studied in pH-7.0 PBS containing 1.0 mmol L^{-1} ATCl by DPV. As shown in **Fig. 6 A**, the current response of all biosensors enhanced with the increase of pH and reached a maximum at pH 7.0. **Fig. 6 B** displayed the effect of AChE loading on the biosensor response. It was

noticed that the DPV peak current increased with increasing the amount of AChE. When the amount of AChE loading on the C_8-MWCNTs/AChE/GCE, SH-MWCNTs/AChE/GCE, IL_1-MWCNTs/AChE/GCE was 0.125 U, 0.125 U, 0.25 U, peak current reached the maximum. Further increase of AChE led to an obvious decrease of current response. It was probably because that the superabundant AChE increased electrode resistance. Hence, 0.125 U, 0.125 U, 0.25 U of AChE was chosen as optimal enzyme concentration for C_8-MWCNTs/AChE/GCE, SH-MWCNTs/AChE/GCE, IL_1-MWCNTs/AChE/GCE, respectively.

Effect of inhibition time on biosensor was investigated. The biosensor was incubated in 1.0×10^{-9} mol L^{-1} OPs standard solution for different time. As show in **Fig. 6 C**, the inhibition rate showed obvious enhancement with increasing time. However, there was no obvious change after reaching equilibration. It was found that optimum inhibition time of C_8-MWCNTs/AChE/GCE, SH-MWCNTs/AChE/GCE, IL_1-MWCNTs/AChE/GCE was 12, 12, 14 min, respectively.

3.4 Detection of standard samples

Fig. 7 showed the calibration plots of OPs. OPs concentration and inhibition rate was linear in the range of 1×10^{-10} to 5×10^{-7} mol L^{-1}. Linear equation of C_8-MWCNTs/AChE/GCE was A=115.96-9.758lgC (R=0.9951). Linear equation of SH-MWCNTs/AChE/GCE was A=147.65-13.322lgC (R=0.9909). Linear equation of IL_1-MWCNTs/AChE/GCE was A=100.13-9.335lgC (R=0.9919). The detection limits of C_8-MWCNTs/AChE/GCE, SH-MWCNTs/AChE/GCE, IL_1-MWCNTs/AChE/GCE were 5.4×10^{-11}, 4.6×10^{-11} and 3.3×10^{-11} mol L^{-1}, respectively. The performance of biosensors and other reported AChE biosensors in the literature [21, 22, 23, 24] was

shown in **Table 1**. Compared with other enzyme electrode sensors, biosensors in this study exhibited wider linear range, lower detection limits and stronger sensitivity.

3.5 Detection of real sample

The biosensor reliability was tested. Different concentrations of OPs were sprayed to fresh vegetable. The concentration of OPs in the vegetable was measured by above prepared enzyme electrodes (See section 2.6). The recovery and relative standard deviations were shown in **Table 2**. For C_8-MWCNTs/AChE/GCE detection, the recoveries were found to be between 94.0% and 102.0%. For SH-MWCNTs/AChE/GCE detection, the recoveries were found to be between 86.0% and 106.0%. For IL_1-MWCNTs/AChE/GCE detection, the recoveries were found to be between 90.0% and 104%. The results indicated that the proposed biosensor was acceptably accurate and precise, and can be used for the analysis of samples from a real environment.

3.6 Reproducibility and Storability of biosensors

Five different modified electrodes of IL_1-MWCNTs/AChE/GCE were used to detect OPs in PBS containing 1.0 mmol L^{-1} ATCl with DPV at above optimum condition. Relative standard deviation (RSD) of peak current was 4.07%. RSD of C_8-MWCNTs/AChE/GCE and SH-MWCNTs/AChE/GCE were 4.31% and 3.45%, respectively. This showed that the reproducibility of three biosensors were better.

The prepared enzyme electrode sensor was stored in an environment of 4 °C and tested once every week in pH-7.0 ATCl solution containing 1.0 mmol L^{-1} (See section 2.3). The peak current signal was recorded and showed in **Fig. 8**. By comparing the peak detection current, we found that the peak current signal remained above 98.5%

within two weeks. With the increase of time, the enzyme activity obviously weakened. After seven weeks, the C_8-MWCNTs/AChE/GCE, SH-MWCNTs/AChE/GCE, IL_1-MWCNTs/AChE/GCE detection signals were 30.50%, 43.40% and 55.70% of the initial peak current, respectively. This showed that the enzyme electrode had good stability and long service life within seven weeks.

4. Conclusion

In this study, MWCNTs as AChE carrier were modified by introducing different functional groups (-SH, $-NH_2$, -Cl), different hydrophobic alkyl groups ($-C_1$, $-C_3$, $-C_8$, $-C_{16}$) and different ionic liquids (IL_1, IL_2). Results showed that MWCNTs surface introducing $-IL_1$ group could be the best carriers for ACHE. IL_1-MWCNTs/AChE/GCE was used to detect OPs and the detection limit was 3.3×10^{-11} mol L^{-1}. At optimum reaction condition (pH 7.0, AChE loading 0.25 U, Inhibition time 14 min), reproducibility test demonstrated that relative standard deviation (RSD) of IL_1-MWCNTs/AChE/GCE was 4.07%. Storability test indicated reactivity of IL_1-MWCNTs/AChE/GCE remained above 98.5% within two weeks. For Real sample detection, the recoveries of IL_1-MWCNTs/AChE/GCE were found to be between 90.0% and 104%. These results demonstrated biosensors in this study exhibited wider linear range, lower detection limits and stronger sensitivity. This work is expected to contribute to the efficient detection of OPs.

Acknowledgments

The work was funded by the National Natural Science Foundation of China (No. 21406093), the Natural Science Foundation of Jiangsu province (BK20140529), Key

University Science Research Project of Jiangsu Province (14KJB530001), China Postdoctoral Science Foundation (2014M550271), and Priority Academic Program Development of Jiangsu Higher Education Institutions.

Compliance with Ethical Standards

Conflict of Interest: Bin Zou declares that he has no conflict of interest. Yanhong Chu declares that she has no conflict of interest. Jiaojiao Xia declares that she has no conflict of interest. Jing Yao declares that she has no conflict of interest.

Ethical Approval: This article does not contain any studies with human participants or animals performed by any of the authors.

Informed Consent: Not applicable.

References

[1]P.B.A. Fai, J.S. TKinfack, Y.J.T. Towa, Acute effects of binary mixtures of Type II pyrethroids and organophosphate insecticides on Oreochromis niloticus [J], Ecotoxicology. 5 (2017) 1-13.

[2] M.E. Millenson, J.M. Braun, A.M. Calafat, D.B. Barr, Y.T. Huang, A. Chen, Urinary organophosphate insecticide metabolite concentrations during pregnancy and children's interpersonal, communication, repetitive, and stereotypic behaviors at 8 years of age: the home study [J], Environ Res. 157 (2017) 9-16.

[3] J. Yu, Y. Ni, M. Zhai, Highly selective non-enzyme glucose detection based on Co-CoO-Co_3O_4 nanocomposites prepared via a solution-combustion and subsequent heat-treating route [J], J Alloy Compd. 723 (2017) 904-911.

[4] R.R. Dutta, P. Puzari, Amperometric biosensing of organophosphate and organocarbamate pesticides utilizing polypyrrole entrapped acetylcholinesterase electrode [J], Biosens Bioelectron. 52 (2014) 166-172.

[5] Y. Liang, C. Qu, R. Yang, Molecularly imprinted electrochemical sensor for daidzein recognition and detection based on poly(sodium 4-styrenesulfonate) functionalized grapheme [J], Sensor Actuat B Chem. 251 (2017): 542-500.

[6] Y. Sun, Y. Wang, J. Li, C. Ding, Y. Lin, W. Sun, An ultrasensitive chemiluminescence aptasensor for thrombin detection based on iron porphyrin catalyzing luminescence desorbed from chitosan modified magnetic oxide graphene composite [J], Talanta. 174 (2017) 809-818.

[7] T. Luo, J. Ke, Y. Xie, Y. Dong, Determination of underivatized amino acids to evaluate quality of beer by capillary electrophoresis with online sweeping technique [J], J Food Drug Anal. 33 (2017) 789-797.

[8] A. Márquez, C. Jiménez-Jorquera, C. Domínguez, X. Muñoz-Berbel, Electrodepositable alginate membranes for enzymatic sensors: an amperometric glucose biosensor for whole blood analysis [J], Biosens Bioelectron. 97 (2017) 136-142.

[9] Y. Shen, G. Shen, Y. Zhang, C. Zhang, H. Li, A novel label-free electrochemical immunosensor based on

aldehyde-terminated ionic liquid [J], Talanta 175 (2017) 347-351.

[10] Z.G. Yu, R.Y. Lai, A reagentless and reusable electrochemical aptamer-based sensor for rapid detection of ampicillin in complex samples [J], Talanta. 44 (2017) 619-624.

[11] L. Xiong, T. Lu, S. Dandan, L. Yan, G. Faming, Bimetallic Pd@Au nanorods based ultrasensitive acetylcholinesterase biosensor for determination of organophosphate pesticides. Sensors & Actuators B Chemical. 255 (2018) 2575-2581.

[12] S. Çevik, S. Timur, Anik Ülkü, Poly(allylamine hydrochloride) functionalized multiwalled carbon nanotube modified carbon paste electrode as acetylcholinesterase biosensor transducer [J], Electroanal. 25 (2013) 2377-2383.

[13] T.W. Kang, S.J. Jeon, H.I. Kim, J.H. Park, D.B. Yim, H.R. Lee, Optical detection of enzymatic activity and inhibitors on non-covalently functionalized fluorescent graphene oxide [J], Acs Nano. 10 (2016) 5-14.

[14] M. Naffakh, A.M. Díez-Pascual, C. MarcoOpportunities and challenges in the use of inorganic fullerene-like nanoparticles to produce advanced polymer nanocomposites [J], Prog Polym Sci. 38 (2013) 1163-1231.

[15] B. Liu, L. Lu, C. Liu, Immunosensor for Myeloperoxidase Based on PoPD-MWCNTs-Ionic Liquid/Nanogold Modified Au Electrode [J], Acta Chim Sinica. 69 (2011) 438-444.

[16] M. D'Aquino, S. Gaetani, M.A. Spadoni, Effect of isouramil on -SH groups and on membrane proteins of riboflavin and tocopherol deprived rat erythrocyte [J], Biochem Soc T. 9 (1981) 356-360.

[17] H.K. Lim, H. Kim, The mechanism of room-temperature ionic-liquid-based electrochemical CO_2 reduction: a review [J], Molecules. 4 (2017) 534-572.

[18] Y.C. Chou, T.F. Hsieh, Y.C. Hsieh, Comparisons of MWCNTs and acidified process by HNO_3, on thermal stability by DSC and TG-FTIR [J], J Therm Anal Calorim. 102 (2010) 641-646.

[19] W. Lei, H.E. Zhen, Z. Bo, Polymerization Mechanism of C-S-H: Identified by FTIR and NMR [J], J Build Mater. 14 (2011): 447-451.

[20] G. Bellussi, R. Millini, E. Montanari, A highly crystalline microporous hybrid organic-inorganic aluminosilicate resembling the AFI-type zeolite [J], Chem Commun. 48 (2012) 7356-7389.

[21] N. Dimcheva, E. Horozova, Y. Ivanov, Self-assembly of acetylcholinesterase on gold nanoparticles electrodeposited on graphite [J], Cent Eur J Chem. 11 (2013) 1740-1748.

[22] Q. Long, H. Li, Y. Zhang, S. Yao, Upconversion nanoparticle-based fluorescence resonance energy transfer assay for organophosphorus pesticides [J], Biosensors & Bioelectronics. 68 (2015) 168-174.

[23] B. Kaur, R. Srivastava, B. Satpati, Nanocrystalline Titanosilicate–Acetylcholinesterase Electrochemical Biosensor for the Ultra- Trace Detection of Toxic Organophosphate Pesticides [J], Chemelectrochem. 2 (2015): 1164-1173.

[24] R. Sundarmurugasan, M.B. Gumpu, B. Ramachandra, Simultaneous detection of monocrotophos and dichlorvos in orange samples using acetylcholinesterase–zinc oxide modified platinum electrode with linear regression calibration [J], Sensors & Actuators B Chemical. 230 (2016) 306-313.

Figure and table captions:

Scheme 1 Illustration of MWCNTs modified by groups.

Scheme 2 Illustration of IL_1-MWCNTs and IL_2-MWCNTs synthesis.

Scheme 3 Illustration of biosensor synthesis.

Fig. 1 DPV of the modified electrode in pH 7.0 PBS solution containing 1.0 mmol L^{-1} ATCl. The curves A, B, C, D were obtained by C_8-MWCNTs, C_3-MWCNTs, C_1-MWCNTs, C_{16}-MWCNTs. The curves E, F, G were obtained by SH-MWCNTs, NH_2-MWCNTs, Cl-MWCNTs. The curves H、I were obtained by IL_1-MWCNTs，IL_2-MWCNTs.

Fig. 2 CVs of modified MWCNTs recorded in pH 7.0 PBS solution containing 5 mmol L^{-1} $[Fe(CN)_6]^{3-/4-}$ and 0.1 mol L^{-1} KCl: (a) bare GCE; (b) MWCNTs/GCE; (c) SH-MWCNTs/GCE; (d) C_8-MWCNTs/GCE; (e) IL_1-MWCNTs/GCE.

Fig. 3 TEM of MWCNTs (A, C) and IL_1-MWCNTs (B, D).

Fig. 4 FTIR of MWCNTs (a), C_8-MWCNTs (b), SH-MWCNTs (c) and IL_1-MWCNTs (d).

Fig. 5 Thermal analysis of MWCNTs (a), C_8-MWCNTs (b), SH-MWCNTs (c), IL_1-MWCNTs (d), C_8-MWCNTs/AChE (e), SH-MWCNTs/AChE (f), IL_1-MWCNTs/AChE (g).

Fig. 6 Effect of pH (A), AChE loading (B), Inhibition time (C) (curve a represents IL_1-MWCNTs, curve b represents SH-MWCNTs, and curve c represents C_8-MWCNTs.).

Fig. 7 Relationship between inhibition rate and OPs. (a) SH-MWCNTs/AChE/GCE; (b) C_8-MWCNTs/AChE/GCE; (c) IL_1-MWCNTs/AChE/GCE.

Fig.8 Enzyme activity rate of C_8-MWCNTs/AChE/GCE, SH-MWCNTs/AChE/GCE, IL_1-MWCNTs/AChE/GCE compared with the initial peak current containing 0.5 mmol/L ATCl phosphate buffer solution.

Table 1 Comparison with other reported biosensors for OPs detection.

Table 2 Determination of OPs in the real sample.

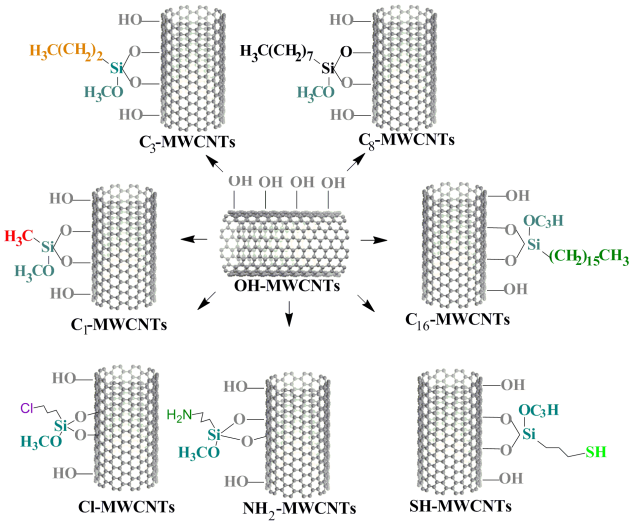

Scheme 1

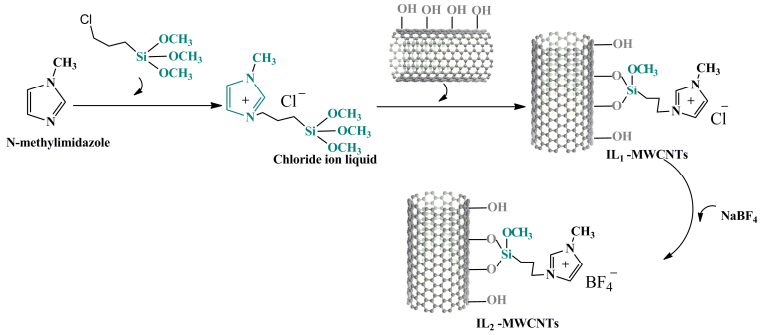

Scheme 2

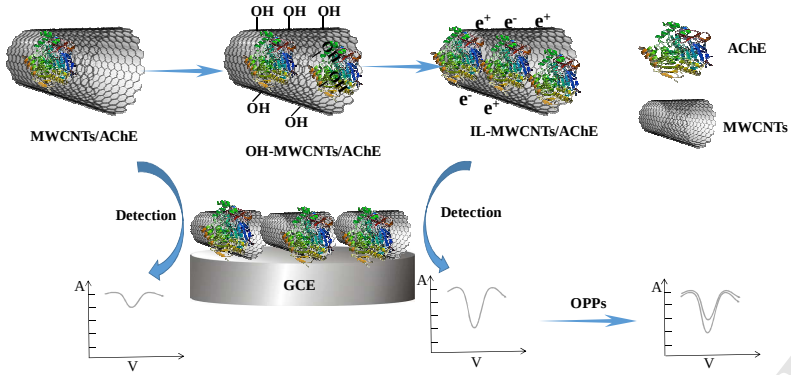

Scheme 3

1

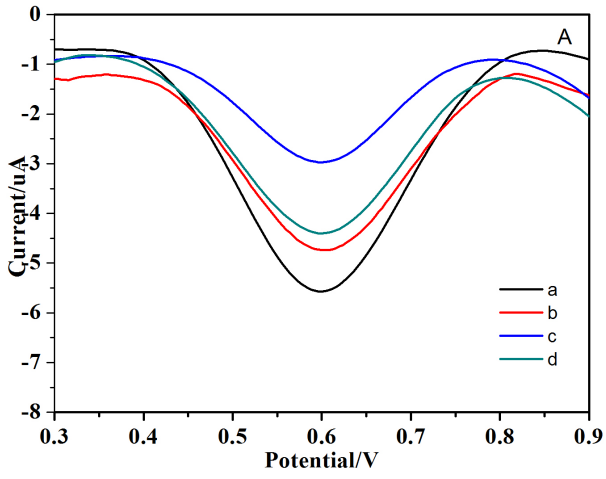
A
Current/uA
Potential/V
a
b
c
d

2

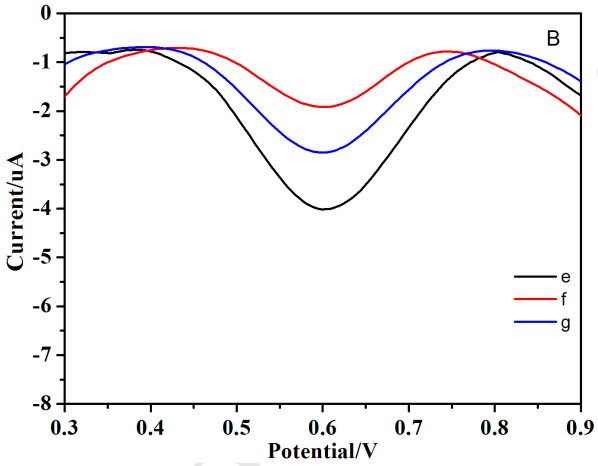
B
Current/uA
Potential/V
e
f
g

3

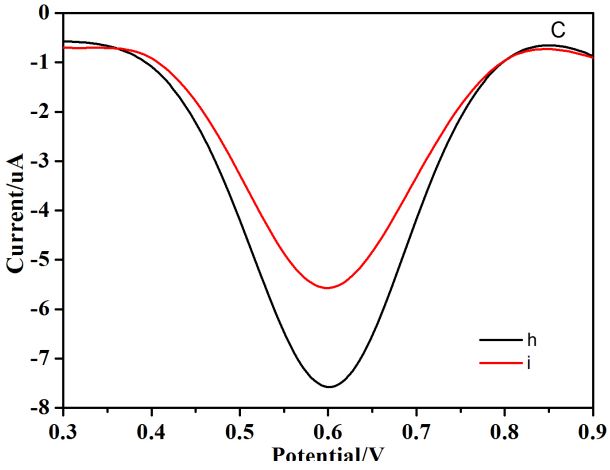
C
Current/uA
Potential/V
h
i

4 **Fig. 1**

5

6

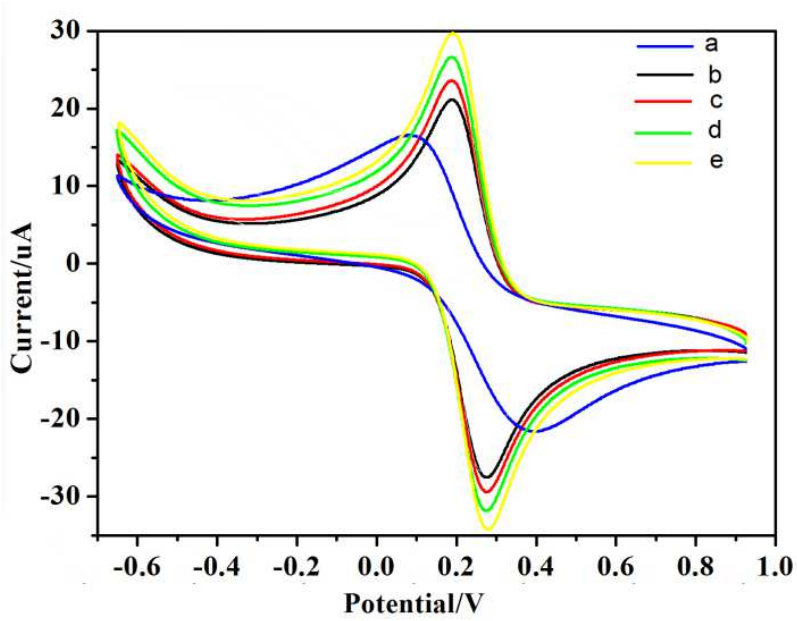

Fig. 2

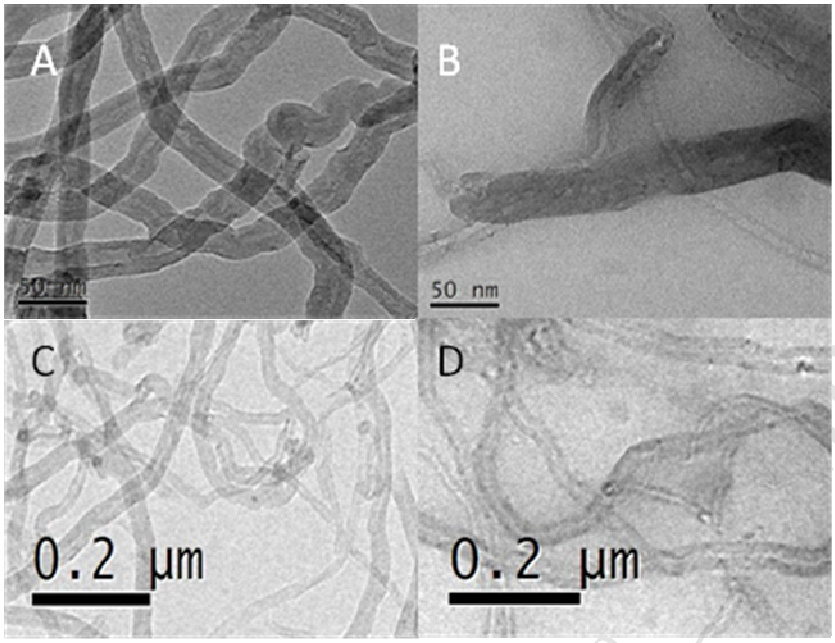

Fig. 3

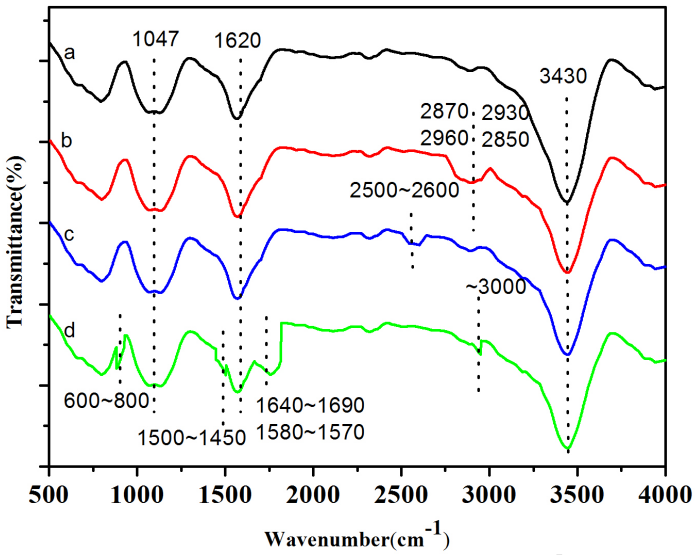

Fig. 4

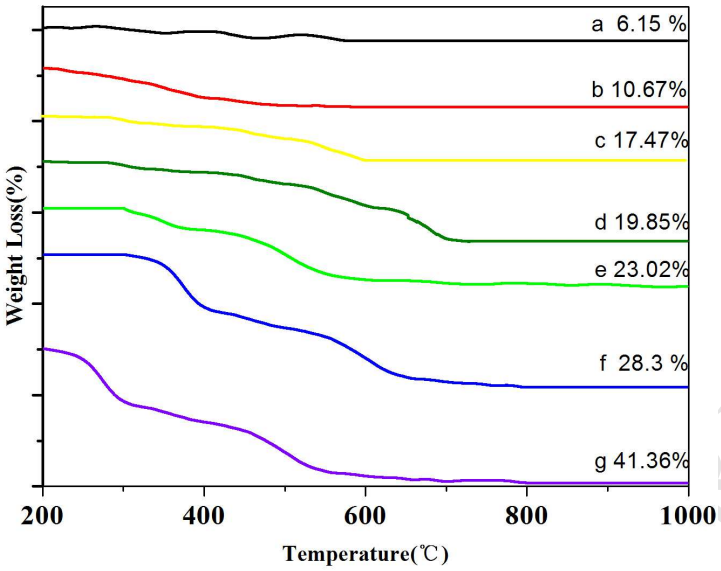

Fig. 5

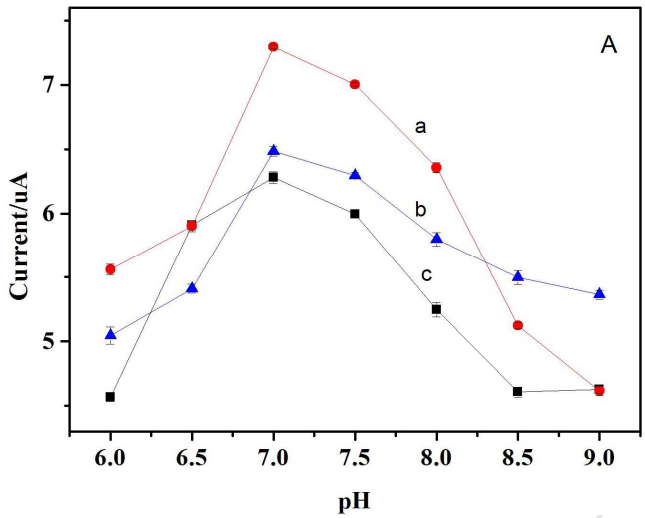
A
a
b
c
Current/uA
pH
7
6
5
6.0
6.5
7.0
7.5
8.0
8.5
9.0

1

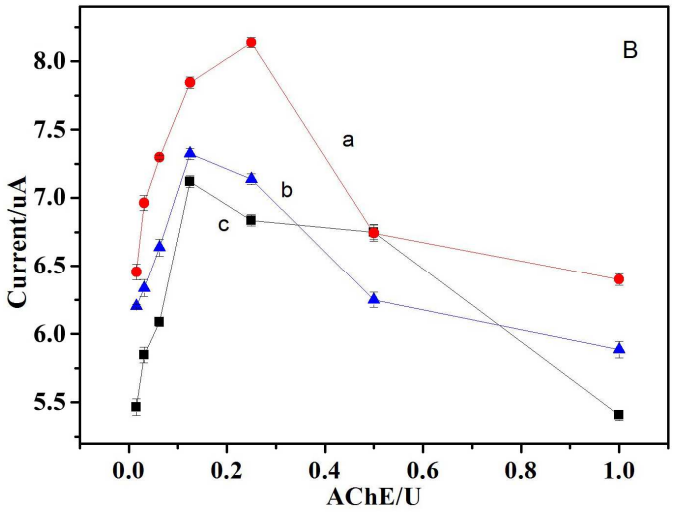
B
a
b
c
Current/uA
AChE/U
8.0
7.5
7.0
6.5
6.0
5.5
0.0
0.2
0.4
0.6
0.8
1.0

2

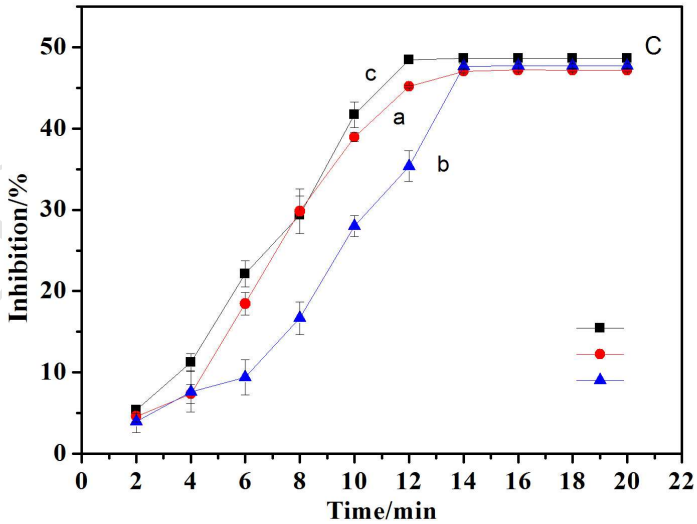
C
c
a
b
Inhibition/%
Time/min
50
40
30
20
10
0
0
2
4
6
8
10
12
14
16
18
20
22

3

4 **Fig. 6**

5

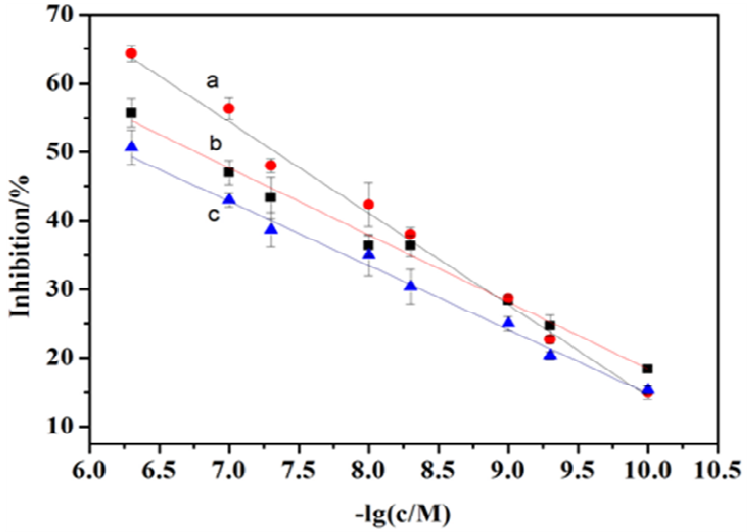

Fig. 7

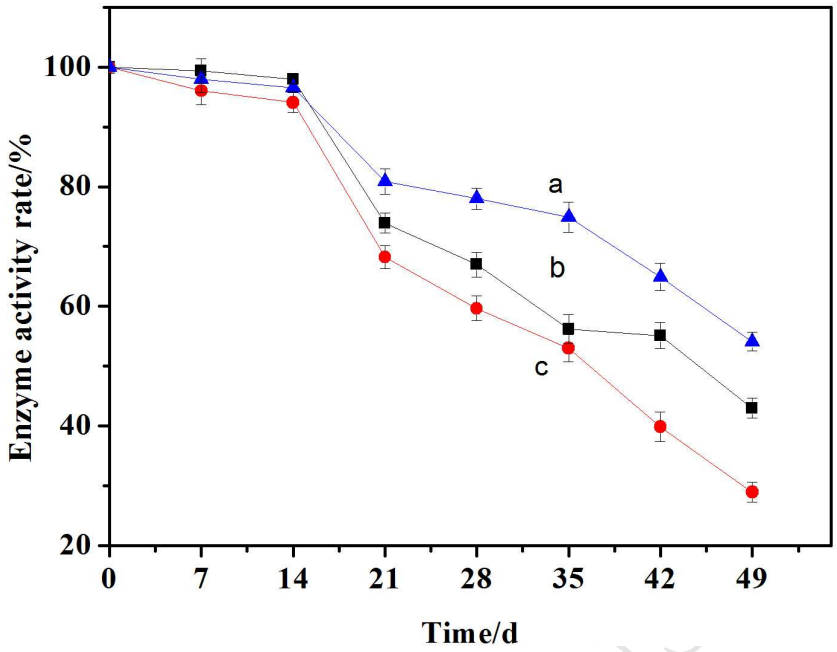

Fig. 8

1 **Table 1** Comparison with other reported biosensors for OPs detection.

Electrode material	Linear range (mol L^{-1})	Detection limit (mol L^{-1})	Analyte	Ref.
AChE/Au/graphite	5.0×10^{-5}-4.0×10^{-4}	5.0×10^{-5}	OPs	Dimcheva et al. 2013
UCNPs-AuNPs-AChE	1×10^{-13}-5×10^{-8}	1.0×10^{-10}	OPs	Long et al. 2015
AChE/Nano-TS-1-Pr-NH_2/GCE	3.6×10^{-10}-3.1×10^{-6}	4.5×10^{-11}	OPs	Kaur et al. 2015
Pt/ZnO/AChE/Chitosan	5×10^{-8}-4×10^{-7}	3.6×10^{-11}	OPs	Sundarmurugasan et al. 2016
IL_1-MWCNTs/AChE/GCE	1.0×10^{-10}-5.0×10^{-7}	3.3×10^{-11}	OPs	This work

2

3

4

5

1 **Table 2** Determination of OPs in the real sample.

	Sample	Added (mol L^{-1})	Found (mol L^{-1})	Mean recovery (%)	RSD(%)（n=3）
C_8-MWCNTs/AChE/GCE	1	5.0×10^{-7}	5.1×10^{-7}	102.0	4.6
	2	5.0×10^{-8}	4.8×10^{-8}	96.0	3.5
	3	5.0×10^{-9}	4.7×10^{-9}	94.0	4.8
SH-MWCNTs/AChE/GCE	1	5.0×10^{-7}	4.3×10^{-7}	86.0	3.9
	2	5.0×10^{-8}	5.2×10^{-8}	104.0	3.3
	3	5.0×10^{-9}	5.3×10^{-9}	106.0	3.7
IL_1-MWCNTs/AChE/GCE	1	5.0×10^{-7}	5.2×10^{-7}	104.0	4.9
	2	5.0×10^{-8}	4.5×10^{-8}	90.0	3.6
	3	5.0×10^{-9}	4.9×10^{-9}	98.0	3.9

2

- Surface modified MWCNTs as carrier to prepare AChE sensors for detection of OPPs
- MWCNTs surface were modified by introducing nine kinds of functional groups.
- It was demonstrated that MWCNTs modified by ionic liquid was the best carrier.
- The detection limit of IL_1/AChE/GCE was 3.3×10^{-11} mol L^{-1}